

Benchmarking inscribed matter probes

Michael Hippke

Sonneberg Observatory, Sternwartestr. 32, 96515 Sonneberg, Germany

Paul Leyland

Brnikat Ltd, 19a Hauxton Road, Little Shelford, Cambridge, CB22 5HJ, United Kingdom

John G. Learned

High Energy Physics Group, Department of Physics and Astronomy, University of Hawaii, Manoa 327 Watanabe Hall, 2505 Correa Road Honolulu, Hawaii 96822 USA

Abstract

We have explored the optimal frequency of interstellar photon communications and benchmarked other particles as information carriers in previous papers of this series. We now compare the latency and bandwidth of sending probes with inscribed matter. Durability requirements such as shields against dust and radiation, as well as data duplication, add negligible weight overhead at velocities $v < 0.2c$. Probes may arrive in full, while most of a photon beam is lost to diffraction. Probes can be more energy efficient per bit, and can have higher bandwidth, compared to classical communication, unless a photon receiver is placed in a stellar gravitational lens. The probe's advantage dominates by order of magnitude for long distances (kpc) and low velocities ($< 0.1c$) at the cost of higher latency.

1. Introduction

Sending a physical artifact can be the most energy-efficient choice for interstellar communications, because it can be done at almost arbitrarily low velocities, and thus low energies. An artifact can arrive at the destination in total, in contrast to a particle beam which is wider than the receiver in all

Email addresses: michael@hippke.org (Michael Hippke), paul@brnikat.com (Paul Leyland), jgl@phys.hawaii.edu (John G. Learned)

realistic cases, so that most energy is lost. The obvious disadvantage is the large communication delay, e.g. sending a probe at a (relatively fast) $0.01 c$ takes 438 years to the nearest star, Proxima.

While such communications have been described in the literature before (e.g., Rose and Wright, 2004), they have never been rigorously examined in terms of data rate, bit per energy, latency, or durability. In this study, we benchmark the inscribed matter probes to optimal photon communication at keV energies (Hippke and Forgan, 2017).

There are two main use cases for inscribed matter. The first is the placement of an artifact in a stellar system to be found at a later time, after the rise of a civilization and its exploration of the system. This scenario is similar to Arthur C. Clarke’s moon monolith (Clarke, 1953). It was suggested to search the solar system for non-terrestrial artifacts (Bracewell, 1960; Papagiannis, 1995; Tough and Lemarchand, 2004; Haqq-Misra and Kopparapu, 2012), particularly for starships (Martin and Bond, 1980) in addition to classical SETI (Gertz, 2016). In our solar system, probes are speculated to be in geocentric, selenocentric, Earth-Moon libration, and Earth-Moon halo orbits (Freitas and Valdes, 1980; Valdes and Freitas, 1983; Freitas, 1983). Alternative ideas include the Kuiper belt (Loeb and Turner, 2012), general technosignatures (Wright, 2017), or even “footprints of alien technology on Earth” (Davies, 2012). A galactic library of knowledge would ease the need for fast communication, keeping the impatient Aliens busy while waiting for the first “answer” from the stars.

The second type is to establish a “live” communication between two distant species using one, or many, probes with onboard storage. In the case that the receiver needs to decelerate such a probe, it appears sensible to first establish contact using faster communication, e.g. using low data rate photons, perhaps even as a beacon. High data rate (high latency) probe exchange can follow after exchanging ephemerides and other protocol details (Hippke and Forgan, 2017).

2. Durability

Space is not empty, but contains a low density of particles, mainly a plasma of hydrogen and helium atoms as well as electromagnetic radiation, magnetic fields, neutrinos, and dust. A probe traveling between the stars will be impacted and potentially damaged by these particles and photons. We now estimate the required shielding and remaining damage.

2.1. Front shield

Heads-on interaction with gas and dust in the interstellar medium at relativistic velocities erodes the front surface and produces craters due to explosive evaporation of surface atoms. Gas penetrates the front to a certain depth.

The erosion from dust impacts has been estimated as 0.1 mm (0.5 mm) for quartz material at $v = 0.1 c$ ($0.2 c$) per pc (Hoang et al., 2017). For the penetration depth of protons there are different estimates between 3 mm in quartz or graphite (at $0.2 c$, Hoang et al., 2017) and 10 mm in titanium (at $0.1 c$, Semyonov, 2009). Penetration depth is a strong function of velocity with a minimum requirement of 10 m of titanium shielding at $v = 0.995$.

Conservatively, the front shield should have a thickness of order $1 + 0.1d$ cm where d is the travel distance in pc (for $v = 0.1 c$). This assures that sufficient proton shielding remains after dust impact erosion towards the end of the journey.

2.2. Side and bottom shields

For dust impacting from the sides, lower velocities in the rest frame of the craft are expected (planetary, km s^{-1}) with typical grain sizes of order μm . This erosion has been determined on average as $22 \mu\text{m } 10^6 \text{ yr}^{-1}$ for iron meteorites in the solar system (Schaeffer et al., 1981) and 6 orders of magnitude lower in interstellar space (Mann, 2010).

These low levels of erosion are dominated by single large impacts. The largest expected particles are of μm sizes, and it is unlikely ($< 1\%$) for a spacecraft to be hit by dust $> 5 \mu\text{m}$ on a decade-long interstellar trip (Poppe, 2016; Hoang et al., 2017). Experimental data for olivine particles with sizes of $0.3 - 1.2 \mu\text{m}$ accelerated towards an aluminum alloy (AlMg_3) at velocities of $3 - 7 \text{ km s}^{-1}$ show deepest craters of $1.64 \mu\text{m}$ (Li et al., 2014). The crater depth is approximately linear with impact velocity between 2 and 8 km s^{-1} and can be extrapolated with hydrocode modeling to depths of $15 \mu\text{m}$ for $2 \mu\text{m}$ -sized particles at 10 km s^{-1} (Price et al., 2012). Based on these estimates, it appears reasonable to design for a wall thickness of e.g., $150 \mu\text{m}$ (giving some safety margin) in aluminum. On average, such a shield will hold for 10^5 yrs based on the $10^{-9} \text{ m yr}^{-1}$ erosion.

2.3. Cosmic ray shielding

In addition, the probe will be hit from all sides by cosmic rays. These are mostly hydrogen and helium nuclei accelerated to relativistic energies.

At low Lorentz factors (< 0.3) we can neglect the anisotropy caused by the probe's velocity. The flux can be approximated by monoenergetic nucleons with an average energy of 1 GeV and its rate is ≈ 11 nucleons $\text{cm}^{-2} \text{s}^{-1}$ (Semyonov, 2009).

Shielding against GeV particles is more effective when using light elements such as polyethylene (CH_2 , $\rho = 0.94 \text{ g cm}^{-3}$) compared to aluminum because of fewer secondary cascades. Still, CH_2 shielding is relatively ineffective. A recent study by Guetersloh et al. (2006) found that only 10% of particles are stopped using a shield depth of 3 cm. When increasing the shield to 10 cm, the absorbed fraction increases to 30%. The further relation between shield thickness and dose reduction is however not linear, and particle shields of close to 100% effectiveness would require depths of several meters, which would result in prohibitively high masses. It appears preferable not to add extra shielding against cosmic rays, but instead invest the mass into error correction.

2.4. Theoretical defects from cosmic ray hits

For a cm-sized probe, most ($> 90\%$) of cosmic rays will pass right through the payload, so that $P \approx 0.1$ of the incoming particles produce primary recoils. Those that interact with the mass, however, will change the arrangement of the atoms in the crystal lattice. This radiation damage can be quantified with displacement theory. The primary knock-on atom moves through the lattice producing a collision cascade, which ends after the collision energy is smaller than the required minimum displacement energy. To estimate the radiation damage, we take an average flux of monoenergetic GeV nucleons at a rate of $F_{\text{nucleons}} \approx 11 \text{ cm}^{-2} \text{ s}^{-1}$ (Semyonov, 2009). This flux is given per unit surface area. A solid physical body, e.g. a dice, has three spatial surfaces, so that a body of volume 1 cm^3 collects $3F_{\text{nucleons}}$ per unit time and volume.

With these estimates, the number of cascades is $P \times 3F_{\text{nucleons}} \approx 0.1 \times 3 \times 11 \approx 3.3 \text{ s}^{-1} \text{ cm}^{-3}$. Over the course of a year, this corresponds to $\approx 10^8$ hits per cm^3 . Each cascade displaces $< 10^3$ atoms for primary hits of GeV energy in most materials (Was, 2017). The total effect is then $< 10^{11}$ displaced atoms per year. This is a small fraction of the total number of 10^{23} atoms per cm^3 .

Each displacement event will erase at most a few bits of information by modifying the chemical structure. Living organisms employ repair enzymes to cope with similar structural damage. A probe could in principle

use nanobots but this would add mass and complexity. A better approach may be to pass the data-repair task onto the recipients; terrestrial molecular geneticists routinely use the BLAST (Altschul et al., 1990) algorithm to reassemble corrupted information, though BLAST is a very general process and not restricted to reading DNA.

In total, unshielded cosmic rays can destroy only a small fraction of the payload even after long (10^6 yrs) travel times. Most of the information can be protected using error correction schemes and/or duplication, which need to account for the fact that defects will occur in shapes of tunnels and clusters.

2.5. Comparison to panspermia research

Panspermia is the hypothesis that life is distributed by bodies such as asteroids. It makes for an interesting comparison, because DNA can store 5×10^{20} bits g^{-1} (Church et al., 2012). Stability is a function of temperature, and DNA decays quickly above 463 K (Karni et al., 2013). At room temperature, its durability is estimated as 50 yrs (Goldman et al., 2013). At cooler temperatures (286 K), the half-life is estimated as 521 years inside bones (Allentoft et al., 2012). In arctic ice (≈ 250 K), $> 80\%$ could be read after 8×10^4 yrs (Miteva et al., 2015).

In a detailed review, the space radiation damage to different microbes was analyzed as a function of shield thickness and time. Some spores such as *D. radiodurans* were found to withstand a dose of 1,000 Gy, and 10^{-6} of the population would survive 10^6 yrs under minimum (cm) shielding (Mileikowsky et al., 2000).

A probe carrying DNA would require a complete encasement of the DNA to avoid hydrolysis and vacuum damage. The survival time of bacteria due to DNA damage by hydrolysis is of the order 10^5 years, based on available experimental evidence (Karran and Lindahl, 1980). DNA decay by vacuum-caused damage occurs much faster than damage by hydrolysis or radiation, in tens of years (Dose et al., 1991). Unshielded micro-organisms are immediately killed by ultraviolet radiation in the solar system, and survive for $\approx 10^5$ years with minimal shields. Outside of the solar system, the photon flux is $10^{-6} \times$ lower and can thus be neglected. Without repair, half-lives of DNA onboard well-designed probes are $10^5 - 10^6$ yrs.

2.6. Probe geometry and structural integrity

The ideal probe geometry is a long cylinder, because most of the shield mass is required for the front, $M_{\text{front}} = \pi r^2 \rho \times (1 + 0.1d)$ g at $v = 0.1c$. Using

graphite ($\rho = 2.2 \text{ g cm}^{-3}$) in a $r = 1 \text{ cm}$ wide probe to Alpha Cen at $v = 0.1 c$ requires $M_{\text{front}} \sim 9 \text{ g}$.

The mass of the side and bottom shields is $((\pi r^2) + (2\pi r h))\rho(2 \times 10^{-4} \text{ g})$. If a given total shield mass is distributed evenly to the front and to the sides in a cylinder-shaped body, its length would be 150 m (for $r = 1 \text{ cm}$). Such a rod has a total shield mass of $\sim 18 \text{ g}$ and a volume of $\sim 5 \times 10^4 \text{ cm}^3$. If the volume is filled with a storage mass of $\rho = 2.2 \text{ g cm}^{-3}$, the payload mass is $\sim 26 \text{ kg}$. Consequently, the shield mass is only $\approx 10^{-4}$ of the payload mass.

Such a very elongated rod might be unstable during a long-term (kyr, Myr) mission due to tumbling. A more conservative length to width ratio of 1 : 100 (instead of 1 : 15,000) would change the fraction of shield mass per payload only to $\approx 10^{-2}$. Even in this conservative configuration, and with more generous shielding, the energy per bit does not change much. In the simple case where shield mass equals payload mass, the energy per bit increases by a factor of two compared to the values calculated in the following sections.

These calculations neglect the mass required for structural integrity at high accelerations, which might be much larger than the shield mass. If the structure is placed at the outside of the probe, it can serve double duty, so that the pure shield mass is even lower.

Over time, dust hits on the hull will decrease stability and integrity of the structure. The shields will become perforated, and radiation damage will cause brittleness, so that cracks and fractures might form. A detailed analysis of the timescale of these effects is outside of the scope of this paper, but likely $> 10^6$ yrs.

3. Information density

A famous quote by Tanenbaum (1989) highlights the data volume of inscribed matter: “Never underestimate the bandwidth of a station wagon full of tapes hurtling down the highway.”¹ Decades later, “sneakernet” is

¹Back in 1989, a common floppy-disk had a capacity of 1,474,560 bytes in the 3.5-inch format, which had a volume of $90 \times 94 \times 3.3 \text{ mm}$, or 27.918 cm^3 . The world’s largest road vehicles are probably to be found in Australia, with a “K road truck” pulling 6 wagons with a total capacity of $\sim 750 \text{ m}^3$, fitting 27.16 million floppy disks, with a total capacity of 4×10^{13} bytes, or 40 TB. This shows the exponential technological advances in storage technology; the same amount of data can today be saved on 80 Micro-SD cards of 512 GB

still used for high-latency high-bandwidth communication between computer systems. The same idea may be applied to interstellar communication.

Throughout this work, we neglect the energy required to encode the stored information, as it is small compared to transmission (Rose and Wright, 2004).

3.1. Theoretical limit of information per mass

The physical maximum of information that can be stored within a spherical volume is given by the ‘‘Bekenstein bound’’ (Bekenstein, 1972, 1973, 1974), which comes from the entropy of a black hole with the same surface area, and is $S_{\text{BH}} = 2 \times 10^{39} \text{ bits g}^{-1}$. A solution without involving an inconvenient black hole has been found by scaling down solid-state flash memory to single electrons at $S_{\text{SS}} = 3 \times 10^{38} \text{ bits g}^{-1}$ (Kish and Granqvist, 2013).

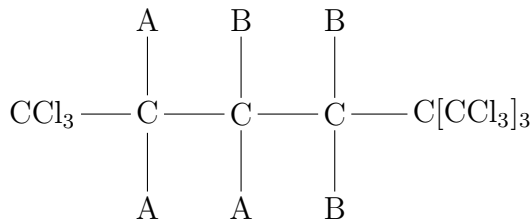
3.2. Nature and current technology

DNA can store $5 \times 10^{20} \text{ bits g}^{-1}$ (Church et al., 2012). Typical proteins encode $2 \times 10^{21} \text{ bits g}^{-1}$ (Sanchez and Grau, 2005). Current technology offers $10^{18} \text{ bits g}^{-1}$ in magnetic hard disks on a thinned 10 nm cobalt layer, and similar values for solid-state disks. Practical disks are much heavier because of durability, read-/write devices, and enclosures.

3.3. Practical limit of information per mass

We now estimate a (conservative, robust) information density limit with ‘‘Earth 2018’’ technology.

Let a tape consist of a long chain of carbon atoms terminated by e.g., a $-\text{CCl}_3$ group at one end and a $-\text{C}(\text{Cl}_3)_3$ group at the other so that the ends of the tape can be distinguished. The actual terminators used could be almost anything, as long as they are distinguishable. Each intervening carbon atom can be bound to a pair of univalent radicals. For simplicity assume that only two different radicals are used, denoted by $-A$ and $-B$. A short tape might then be:



each. These cards are tiny, so that within 27 years, we were able to shrink a gigantic road truck to the size of a golf ball.

An order of magnitude gain in storage density could be reached by encoding more bits per a.m.u. by using e.g., $-H$, $-D$, $-CH_3$, $-CH_2D$, $-CHD_2$ and $-CD_3$ radicals. Such an encoding scheme would allow for 23 states to be encoded in an average of 35 a.m.u each, which corresponds to $35 \times \log_2(23) \approx 7.7$ a.m.u per bit. For simplicity and increased stability, we continue with perfluorinated alkane as an example.

Each carbon atom in the chain can have one of three substitution patterns (the formulae $-CAB-$ and $-CBA-$ are structurally and chemically identical) and can store one trinary digit (tit) or $\log_2(3) \approx 1.6$ bits.

The lowest mass choices for the A and B radicals are $-H$ and $-D$ with masses of 1 and 2 a.m.u. respectively. The atomic mass of carbon is 12 a.m.u. so assuming equal populations of each combination the average mass for this case is 15 a.m.u per tit. Reading and writing the tape would be easier, from a chemical point of view, if A were hydrogen and B were methyl ($-CH_3$) which has a mass of 15 a.m.u. The average mass now becomes 28 a.m.u per tit. Long term chemical stability suggests that rather than hydrogen we should use fluorine atoms, which have a mass of 19 a.m.u, so the average mass per tit rises to 100 a.m.u per tit.

One a.m.u is equal to 1.66×10^{-27} kg, so that the described encoding schemes allow for $S_{\text{chem}} = 6 \times 10^{23}$ bits g^{-1} , or a magnitude less or more depending on the desired stability.

Compared to DNA, perfluorocarbon chemistry provides higher stability at low temperature and in the absence of vicious reagents by orders of magnitude. Its chemistry stops $\lesssim 500$ K, an advantage for the short periods of high temperatures during a laser-pushed launch (Lubin, 2016; Kipping, 2017) and the close stellar encounter of a photogravitational deceleration (Heller and Hippke, 2017; Heller et al., 2017; Forgan et al., 2017).

The enclosure of the probe, structural components, and overhead for error detection and correction codes will make the information payload a fraction of the total probe mass, e.g. 20%. We use $S_{\text{base}} = 10^{23}$ bits g^{-1} in the following sections, and the reader is welcome to favor other values. As Richard Feynman (1992) noted: “There’s plenty of room at the bottom”.

4. Transportation

It is still debated whether there is a lower limit on the minimal energy required per transmitted bit (Porod, 1988; Landauer, 1996). In practice, however, interstellar communication needs to leave our solar system, and

thus massive particles require a minimum speed of $\approx 20 \text{ km s}^{-1}$, the solar system escape velocity. Mass-less particles have comparable energy limits because of thermal noise, as pointed out by Holevo (1973); Giovannetti et al. (2014).

A key advantage of inscribed matter communications is that its energy requirements are independent of distance, instead they are a function of velocity. In contrast, a particle beam’s width widens with distance, making the receiver flux level an inverse quadratic function of distance. While mass-less particles are cheap (there are 5×10^{15} photons per Joule at $\lambda = \text{nm}$), it gives an advantage to matter over photons for larger distances. In any comparison between matter and particle communication there is a distance d_0 after which probes are more energy efficient for a given technology (but require longer wait times).

Theoretically, the kinetic energy invested into accelerating a mass can (almost) be recovered during its deceleration, making such communications extremely energy efficient (Landauer, 1998). In practice, this would require the construction of megastructures in space and is neglected here: We will instead assume that the kinetic energy is required twice.

4.1. Potential transportation scheme

A recent proposal by the “Breakthrough Initiatives” (Lubin, 2016; Popkin, 2017) suggests that near future technology can launch 1 g payloads with a cruise velocity of $0.2c$ using strong lasers. Such a probe would arrive at the nearest star, $\alpha \text{ Cen}$, after about 20 years, corresponding to a data rate of e.g. 10^{18} bits over 20 years, or 10^9 bits per second (Gbit/s). Launching probes regularly, e.g. one per day, increases the effective data rate by orders of magnitude.

4.2. Energy requirements per bit of inscribed matter

Accelerating a probe to velocities v close to the speed of light c requires a relativistic treatment. For slow probes $v \ll c$ we can approximate the Lorentz factor as $L = 1$ with an error of $\approx 5\%$ ($\approx 15\%$, $\approx 100\%$) at $0.3c$ ($0.5c$, $0.9c$), or calculate

$$L = \frac{1}{\sqrt{1 - v^2/c^2}}. \tag{1}$$

The kinetic energy of an object is

$$E_{\text{kin}} = \frac{1}{2}mv^2 \quad (2)$$

where m is the object's mass (in kg), and v its velocity (in m s^{-1}). With η as the propulsion efficiency factor for launch and deceleration, the capacity of the channel is

$$C_{\text{rel}} = \eta S L^{-1} v^{-2} \text{ (bits J}^{-1}\text{)}. \quad (3)$$

With $S_{\text{base}} = 10^{23} \text{ bits g}^{-1}$ and $v = 0.1 c$ we get an energy efficiency of $\approx 10^{11} \text{ bits per Joule}$, where we can neglect the small Lorentz factor ($L = 1.005$).

5. Discussion

5.1. Comparison to photon communications

We can compare matter to the optimal photon communication at $\lambda \approx \text{nm}$ where the number of received particles is (Hippke and Forgan, 2017)

$$\gamma \sim \left(\frac{d}{1 \text{ pc}}\right)^{-2} \left(\frac{D_t}{1 \text{ m}}\right)^2 \left(\frac{D_r}{1 \text{ m}}\right)^2 \left(\frac{P}{1 \text{ W}}\right) \text{ (s}^{-1}\text{)} \quad (4)$$

with d as the distance, D_t and D_r as transmitter and receiver apertures, and P as the transmitter power. Using a conservative capacity of one bit per photon (Hippke, 2017b), setting $D = D_t = D_r$, and dividing by power, we can write the capacity of the channel as a function of wavelength and in units of bits per energy:

$$C_\gamma = \eta \left(\frac{d}{1 \text{ pc}}\right)^{-2} \left(\frac{\lambda}{1 \text{ nm}}\right)^{-1} \left(\frac{D}{1 \text{ m}}\right)^4 \text{ (bits J}^{-1}\text{)}. \quad (5)$$

We can set $C_\gamma = C_{\text{rel}}$ to match the energy efficiency of $10^{11} \text{ bits per Joule}$ as in the inscribed matter case. For $d = 1.3 \text{ pc}$, we require $D = 1 \text{ km}$ at X-ray energy, which is large. For optical lasers ($\lambda = \mu\text{m}$) and microwaves ($\lambda = 0.1 \text{ m}$), the apertures would need to be larger by $10\times$ and $100\times$, respectively.

For a constant wavelength, the apertures must increase with distance d as $D \propto d^{1/2}$. For a constant $v = 0.1 c$, the apertures increase with distances $d = 10 \text{ pc}$ (100 pc, 1,000 pc) to $D = 3 \text{ km}$ (9 km, 27 km).

For low probe speeds ($v \ll 0.01 c$), aperture sizes for energy equivalence become implausibly high. In this regime, inscribed matter is more energy efficient by many orders of magnitude.

5.2. Limits on energy and aperture size

In the real world, the amount of energy used to accelerate (and decelerate) the probe is limited, as is the beamer size. As an example, “Breakthrough Starshot” proposes to use a 100 GW laser with a 10 km aperture, sufficient to accelerate 1 g to $v = 0.2c$. At first approximation, mass and travel time can be traded. At a slower velocity of e.g., $v = 0.002c$, the mass could be 100 g for a travel time to α Cen of 2,000 yrs, which is acceptable with respect to decay. Practical limits on power and aperture impose a limit on mass and velocity. Without megastructures and extreme power levels, masses will plausibly be limited to the kg range.

5.3. Comparison to photon communications through stellar gravitational lenses

Alternatively, meter-scale telescopes could be placed in the gravitational lenses of both stars, achieving an equivalent of 75 km apertures on the receiving legs only (Hippke, 2017a). Using meter-size transmitters, photon communication is more efficient over 1.3 pc compared to a probe with $v = 0.1c$, and achieves parity at kpc distances.

5.4. Decoupling of times

As explained in the introduction, inscribed matter probes can be employed for different purposes. One scenario is to send a library onboard a sentinel with the wishful thinking that something may eventually evolve the capability to read it.

An active “sneakernet”, in contrast, presupposes that a channel set-up protocol has already been established before the first probe is sent. Then, a large bulk of data can be transmitted relatively cheaply without clogging up a bosonic network connection. This scenario resembles today’s occasional transfers of large amounts of data via traditional mail channels, e.g. on disks.

Sending a sentinel also removes the requirement of synchronicity. It allows the sender to decouple the time required for information preparation and transmission. For example, a probe (or many probes) can be assembled in parallel, perhaps consisting of many separate storage chips. Each probe can be sent with a catapult (or photon beamer, etc.) in a relatively short time (minutes). When we compare a g-mass probe (with 10^{23} bits of information), a launch to $0.2c$ would take ≈ 2 minutes, compared to a multi-year transmission campaign for the same amount of data. The quantity of data per unit time can thus be much larger than with a bosonic transmitter, and

can be targeted at many different receivers, as long as energy is not the bottleneck.

In a bosonic channel, sender and receiver must spend the same amount of time, and the same time (plus light travel time) for communication. If the particles are not received, the information is lost forever. As an analogy, the bosonic channel would be a live TV broadcast, while the probe would represent a letter waiting in your mailbox.

5.5. Probe strategies

In principle, and in contrast to the communication strategies discussed in the previous section, no network needs to be established before sending a probe. As an example, the sender of the probe may estimate a relevant chance that a technological species exists, or may evolve in the future, in a target system. The sender can launch a probe with a trajectory to be captured at the destination system e.g., via three-body gravitational interactions involving the probe, a gas giant such as Jupiter, and the star. Interstellar comets, similar to Oumuamua (Meech et al., 2017), are regularly captured by the solar system “fishing net” (Lingam and Loeb, 2018). Alternatively, deceleration with a light sail is possible from a few percent the speed of light, using a photogravimagnetic manoeuvre (Heller and Hippke, 2017; Heller et al., 2017; Forgan et al., 2017). The probe can then be landed on a moon, parked in a stable orbit around Lagrangian points, or may be actively controlled e.g., by an on-board AI.

The efficiency of probes compared to photons is strongly related to the communication distance. If the average distance between species is short, photons might be preferred in many cases. In regions with high stellar densities, such as globular clusters or the galactic center, the average distance between stars is an order of magnitude shorter (Miocchi et al., 2013). If these places are suitable for technological life, they may be dominated by photon communications. In the outskirts of the galaxy, the opposite may be true.

6. Conclusion

Probes which carry inscribed matter have higher latency compared to photon communications; realistic cases are a factor of $10\times$ for $v = 0.1c$. If this delay is acceptable for both sides, inscribed matter is favorable for cases where large amounts of data ($> 10^{23}$ bits) shall be transmitted over a comparably short time (centuries). Its energy efficiency (per bit) increases

with distance compared to photons, and is equivalent to photon communications with large (km) apertures over pc distances. Practical limits due to durability arise for travel times $> 10^6$ yrs, which covers all of the galaxy at $v = 0.1 c$, but makes intergalactic communication prohibitive. Stellar gravitational lensing at the receiver side is more efficient out to kpc, limiting inscribed matter to scenarios such as the long-term deposition of artifacts inside a stellar system.

7. References

References

- Allentoft, M., Collins, M., Harker, D., Haile, J., Oskam, C., Hale, M., Campos, P., Samaniego Castruita, J., Gilbert, T., Willerslev, E., Zhang, G., Scofield, R., Holdaway, R., Bunce, M., 2012. The half-life of dna in bone: measuring decay kinetics in 158 dated fossils. Royal Society of London. Proceedings B. Biological Sciences 279 (1748), 4724–4733.
- Altschul, S. F., Gish, W., Miller, W., Myers, E. W., Lipman, D. J., oct 1990. Basic local alignment search tool. Journal of Molecular Biology 215 (3), 403–410.
URL [https://doi.org/10.1016/s0022-2836\(05\)80360-2](https://doi.org/10.1016/s0022-2836(05)80360-2)
- Bekenstein, J. D., 1972. Black holes and the second law. Nuovo Cimento Lettere 4, 737–740.
- Bekenstein, J. D., Apr. 1973. Black Holes and Entropy. Physical Review D 7, 2333–2346.
- Bekenstein, J. D., Jun. 1974. Generalized second law of thermodynamics in black-hole physics. Physical Review D 9, 3292–3300.
- Bracewell, R. N., May 1960. Communications from Superior Galactic Communities. Nature 186, 670–671.
- Church, G. M., Gao, Y., Kosuri, S., Sep. 2012. Next-Generation Digital Information Storage in DNA. Science 337, 1628.
- Clarke, A., 1953. The Sentinel, in: Expedition to Earth. Ballantyne Books.
- Davies, P. C. W., Apr. 2012. Footprints of alien technology. Acta Astronautica 73, 250–257.
- Dose, K., Bieger-Dose, A., Kerz, O., Gill, M., May 1991. DNA-strand breaks limit survival in extreme dryness. Origins of Life and Evolution of the Biosphere 21, 177–187.
- Feynman, R. P., March 1992. There’s plenty of room at the bottom [data storage]. Journal of Microelectromechanical Systems 1 (1), 60–66.

- Forgan, D. H., Heller, R., Hippke, M., Oct. 2017. Photogravimagnetic assists of light sails: a mixed blessing for Breakthrough Starshot? ArXiv e-prints.
- Freitas, Jr., R. A., Aug. 1983. If they are here, where are they? Observational and search considerations. *Icarus* 55, 337–343.
- Freitas, Jr., R. A., Valdes, F., Jun. 1980. A search for natural or artificial objects located at the earth-moon libration points. *Icarus* 42, 442–447.
- Gertz, J., Aug. 2016. ET Probes: Looking Here as Well as There. ArXiv e-prints.
- Giovannetti, V., García-Patrón, R., Cerf, N. J., Holevo, A. S., Oct. 2014. Ultimate classical communication rates of quantum optical channels. *Nature Photonics* 8, 796–800.
- Goldman, N., Bertone, P., Chen, S., Dessimoz, C., Leproust, E. M., Sipos, B., Birney, E., Feb. 2013. Towards practical, high-capacity, low-maintenance information storage in synthesized DNA. *Nature* 494, 77–80.
- Guetersloh, S., Zeitlin, C., Heilbronn, L., Miller, J., Komiyama, T., Fukumura, A., Iwata, Y., Murakami, T., Bhattacharya, M., 2006. Polyethylene as a radiation shielding standard in simulated cosmic-ray environments. *Nuclear Instruments and Methods in Physics Research Section B: Beam Interactions with Materials and Atoms* 252 (2), 319 – 332. URL <http://www.sciencedirect.com/science/article/pii/S0168583X06008822>
- Haqq-Misra, J., Kopparapu, R. K., Mar. 2012. On the likelihood of non-terrestrial artifacts in the Solar System. *Acta Astronautica* 72, 15–20.
- Heller, R., Hippke, M., Feb. 2017. Deceleration of High-velocity Interstellar Photon Sails into Bound Orbits at α Centauri. *Astrophysical Journal Letters* 835, L32.
- Heller, R., Hippke, M., Kervella, P., Sep. 2017. Optimized Trajectories to the Nearest Stars Using Lightweight High-velocity Photon Sails. *Astronomical Journal* 154, 115.
- Hippke, M., Jun. 2017a. Interstellar communication. II. Application to the solar gravitational lens. ArXiv e-prints.

- Hippke, M., Dec. 2017b. Interstellar communication. V. Introduction to photon information efficiency (in bits per photon). ArXiv e-prints.
- Hippke, M., Forgan, D. H., Nov. 2017. Interstellar communication. III. Optimal frequency to maximize data rate. ArXiv e-prints.
- Hoang, T., Lazarian, A., Burkhart, B., Loeb, A., Mar. 2017. The Interaction of Relativistic Spacecrafts with the Interstellar Medium. *Astrophysical Journal* 837, 5.
- Holevo, A. S., 1973. Bounds for the quantity of information transmitted by a quantum communication channel. *Problemy Peredachi Informatsii* 9 (3), 3–11.
- Karni, M., Zidon, D., Polak, P., Zalevsky, Z., Shefi, O., 2013. Thermal degradation of dna. *DNA and cell biology* 32 6, 298–301.
- Karran, P., Lindahl, T., 1980. Hypoxanthine in deoxyribonucleic acid: generation by heat-induced hydrolysis of adenine residues and release in free form by a deoxyribonucleic acid glycosylase from calf thymus. *Biochemistry* 19 (26), 6005–6011, pMID: 7193480.
URL <http://dx.doi.org/10.1021/bi00567a010>
- Kipping, D., Jun. 2017. Relativistic Light Sails. *Astronomical Journal* 153, 277.
- Kish, L. B., Granqvist, C.-G., Sep. 2013. Does Information Have Mass? ArXiv e-prints.
- Landauer, R., Jun. 1996. Minimal Energy Requirements in Communication. *Science* 272, 1914–1918.
- Landauer, R., Jan. 1998. Energy needed to send a bit. *Proceedings of the Royal Society of London Series A* 454, 305.
- Li, Y. W., Bugiel, S., Tieloff, M., Hillier, J. K., Postberg, F., Price, M. C., Shu, A., Fiege, K., Fielding, L. A., Armes, S. P., Wu, Y. Y., Grn, E., Srama, R., 2014. Morphology of craters generated by hypervelocity impacts of micron-sized polypyrrole-coated olivine particles. *Meteoritics and Planetary Science* 49 (8), 1375–1387.
URL <http://dx.doi.org/10.1111/maps.12338>

- Lingam, M., Loeb, A., Jan. 2018. Implications of Captured Interstellar Objects for Panspermia and Extraterrestrial Life. ArXiv e-prints.
- Loeb, A., Turner, E. L., Apr. 2012. Detection Technique for Artificially Illuminated Objects in the Outer Solar System and Beyond. *Astrobiology* 12, 290–294.
- Lubin, P., Apr. 2016. A Roadmap to Interstellar Flight. ArXiv e-prints.
- Mann, I., 2010. Interstellar dust in the solar system. *Annual Review of Astronomy and Astrophysics* 48 (1), 173–203.
URL <https://doi.org/10.1146/annurev-astro-081309-130846>
- Martin, A. R., Bond, A., 1980. *Starships and their Detectability*. Springer Netherlands, Dordrecht, pp. 197–226.
- Meech, K. J., Weryk, R., Micheli, M., Kleyna, J. T., Hainaut, O. R., Jedicke, R., Wainscoat, R. J., Chambers, K. C., Keane, J. V., Petric, A., Denneau, L., Magnier, E., Berger, T., Huber, M. E., Flewelling, H., Waters, C., Schunova-Lilly, E., Chastel, S., Dec. 2017. A brief visit from a red and extremely elongated interstellar asteroid. *Nature* 552, 378–381.
- Mileikowsky, C., Cucinotta, F. A., Wilson, J. W., Gladman, B., Horneck, G., Lindegren, L., Melosh, J., Rickman, H., Valtonen, M., Zheng, J. Q., Jun. 2000. Natural Transfer of Viable Microbes in Space. 1. From Mars to Earth and Earth to Mars. *Icarus* 145, 391–427.
- Miocchi, P., Lanzoni, B., Ferraro, F. R., Dalessandro, E., Vesperini, E., Pasquato, M., Beccari, G., Pallanca, C., Sanna, N., Sep. 2013. Star Count Density Profiles and Structural Parameters of 26 Galactic Globular Clusters. *Astrophysical Journal* 774.
- Miteva, V., Rinehold, K., Sowers, T., Sebastian, A., Brenchley, J., 2015. Abundance, viability and diversity of the indigenous microbial populations at different depths of the neem greenland ice core. *Polar Research* 34 (1), 25057.
URL <https://doi.org/10.3402/polar.v34.25057>
- Papagiannis, M., 1995. The Search for Extraterrestrial Technologies in our Solar System. In: Shostak, G. S. (Ed.), *Progress in the Search for Extraterrestrial Life*. Vol. 74 of *Astronomical Society of the Pacific Conference Series*. p. 425.

- Popkin, G., Feb. 2017. What it would take to reach the stars. *Nature* 542, 20–22.
- Poppe, A. R., Jan. 2016. An improved model for interplanetary dust fluxes in the outer Solar System. *Icarus* 264, 369–386.
- Porod, W., Jun. 1988. Comment on “Energy requirements in communication” [*Appl. Phys. Lett.* 51, 2056 (1987)]. *Applied Physics Letters* 52, 2191.
- Price, M. C., Kearsley, A. T., Burchell, M. J., HOWARD, L. E., HILLIER, J. K., STARKEY, N. A., WOZNIAKIEWICZ, P. J., COLE, M. J., 2012. Stardust interstellar dust calibration: Hydrocode modeling of impacts on al-1100 foil at velocities up to 300 km s⁻¹ and validation with experimental data. *Meteoritics and Planetary Science* 47 (4), 684–695.
URL <http://dx.doi.org/10.1111/j.1945-5100.2011.01300.x>
- Rose, C., Wright, G., Sep. 2004. Inscribed matter as an energy-efficient means of communication with an extraterrestrial civilization. *Nature* 431, 47–49.
- Sanchez, R., Grau, R., Dec. 2005. The energy cost of protein messages lead to a new protein information law. eprint arXiv:q-bio/0512025.
- Schaeffer, O. A., Nagel, K., Fechtig, H., Neukum, G., Oct. 1981. Space erosion of meteorites and the secular variation of cosmic rays /over 10 to the 9th years/. *Planetary and Space Science* 29, 1109–1118.
- Semyonov, O. G., Mar. 2009. Radiation hazard of relativistic interstellar flight. *Acta Astronautica* 64, 644–653.
- Tanenbaum, A., 1989. *Computer Networks*. Prentice-Hall, New Jersey.
- Tough, A., Lemarchand, G. A., Jun. 2004. Searching for Extraterrestrial Technologies Within Our Solar System. In: Norris, R., Stootman, F. (Eds.), *Bioastronomy 2002: Life Among the Stars*. Vol. 213 of IAU Symposium. p. 487.
- Valdes, F., Freitas, R. A., Mar. 1983. A search for objects near the earth-moon Lagrangian points. *Icarus* 53, 453–457.
- Was, G. S., 2017. *The Displacement of Atoms*. Springer New York, New York, NY, pp. 77–130.

Wright, J. T., Apr. 2017. Prior Indigenous Technological Species. ArXiv e-prints.